Supplementary Materials

All 3D-printed high-sensitivity adaptive hydrogel strain sensor for accurate plant growth monitoring

Lina Wang[1,2,#], Wen Wang[1,#], Rongtai Wan[1,2,#], Mutian Yao[1,2], Wenna Chen[2], Liuyu Zhang[3], Jingkun Xu[1], Ximei Liu[1,2,*], Baoyang Lu[1,2,*]

[1]Jiangxi Provincial Key Laboratory of Flexible Electronics, Jiangxi Science and Technology Normal University, Nanchang 330013, Jiangxi, China.
[2]School of Pharmacy, Jiangxi Science and Technology Normal University, Nanchang 330013, Jiangxi, China.
[3]College of Information Science & Engineering, Shenyang Ligong University, Shenyang 110159, Liaoning, China.
[#]Authors contributed equally.

[*]**Correspondence to:** Prof. Ximei Liu, School of Pharmacy, Jiangxi Science and Technology Normal University, No. 605 Fenglin Avenue, Changbei Economic Development Zone, Nanchang 330013, Jiangxi, China. E-mail: liuxm@jxstnu.edu.cn; Prof. Baoyang Lu, Jiangxi Provincial Key Laboratory of Flexible Electronics, Flexible Electronics Innovation Institute, Jiangxi Science and Technology Normal University, No. 605 Fenglin Avenue, Changbei Economic Development Zone, Nanchang 330013, Jiangxi, China. E-mail: luby@jxstnu.edu.cn

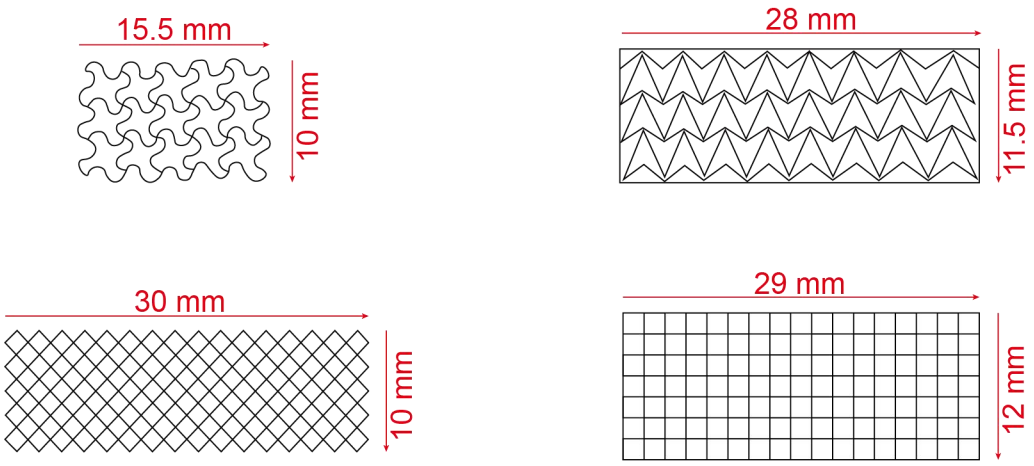

Supplementary Figure 1. Patterns of different conductive layers in SVG format: microwave pattern; curved line; rhombic; square.

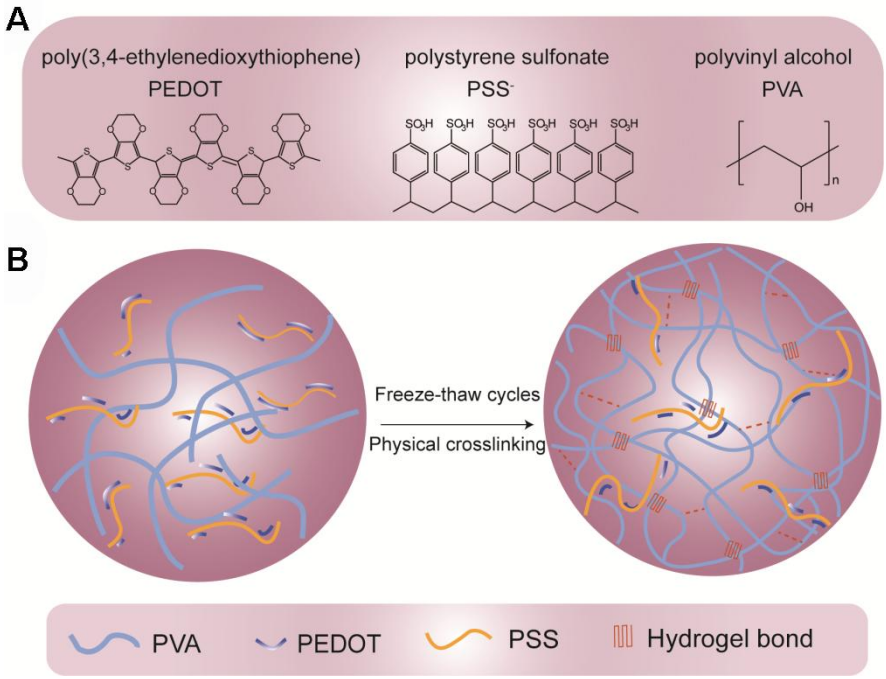

Supplementary Figure 2. Mechanism diagram and the preparation process of PEDOT:PSS-PVA hydrogel. (A) Structural formulae for PEDOT:PSS and PVA. (B) Cross-linking mechanism of PEDOT:PSS-PVA hydrogels.

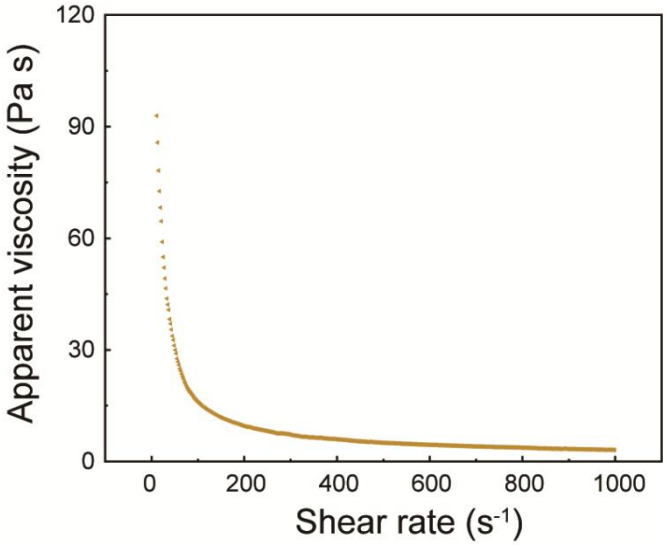

Supplementary Figure 3. Viscosity vs shear rate for PEDOT:PSS-PVA inks.

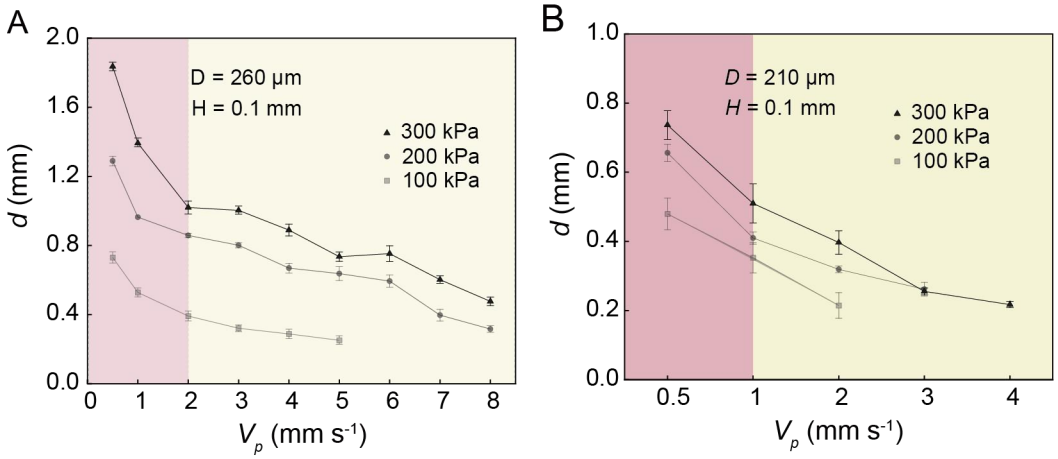

Supplementary Figure 4. Evaluation of Multimaterial Ink Printability. (A) Printed PEDOT:PSS-PVA ink line width vs print speed (0-8 mm s^{-1}) and print pressure (100, 200, 300 kPa) for the print nozzle size of 260 µm and the print height of 0.1mm. (B) Printed PVA ink line width vs print speed (0-6 mm s^{-1}) and print pressure (100, 200, 300 kPa) for the print nozzle size of 210 µm and the print height of 0.1mm.

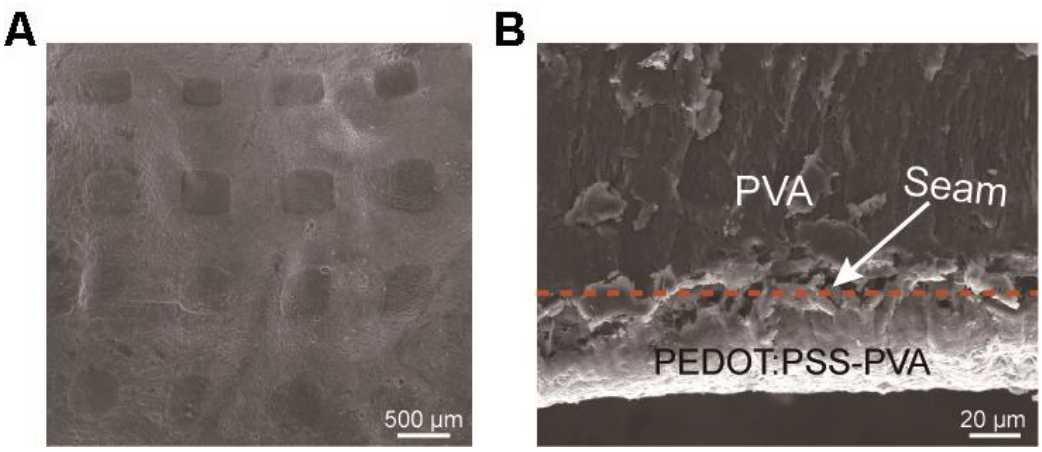

Supplementary Figure 5. (A)Top-view and (B) cross-sectional SEM images of PEDOT:PSS-PVA conductive layer on PVA flexible substrate by 3D printing technique.

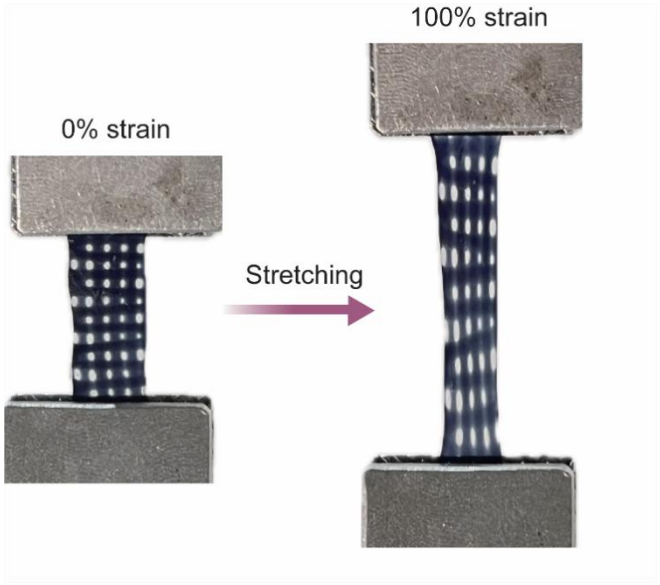

Supplementary Figure 6. 3D Printing Integrated PEDOT:PSS-PVA Hydrogel at 0% and 100% strain Comparison of Physical Plots.

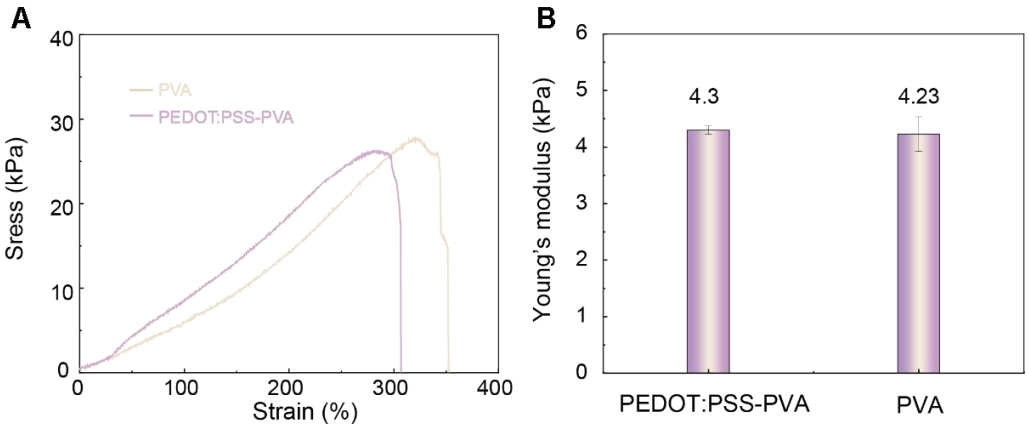

Supplementary Figure 7. Mechanical performance tests. Stress-strain curves (A) and Young's modulus (B) of pure PVA and PEDOT:PSS-PVA.

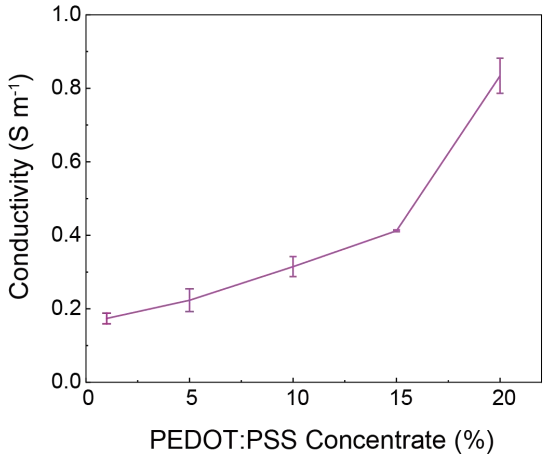

Supplementary Figure 8. Conductivity of PEDOT:PSS conducting hydrogels at different concentrations (1 wt.%, 5 wt.%, 10 wt.%, 15 wt.%, 20 wt.%).

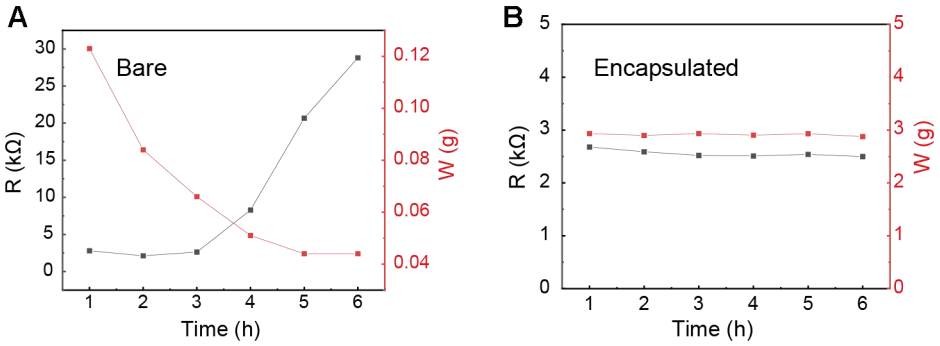

Supplementary Figure 9. Resistance value and mass versus time curves for the bare device (A) and encapsulated device (B).

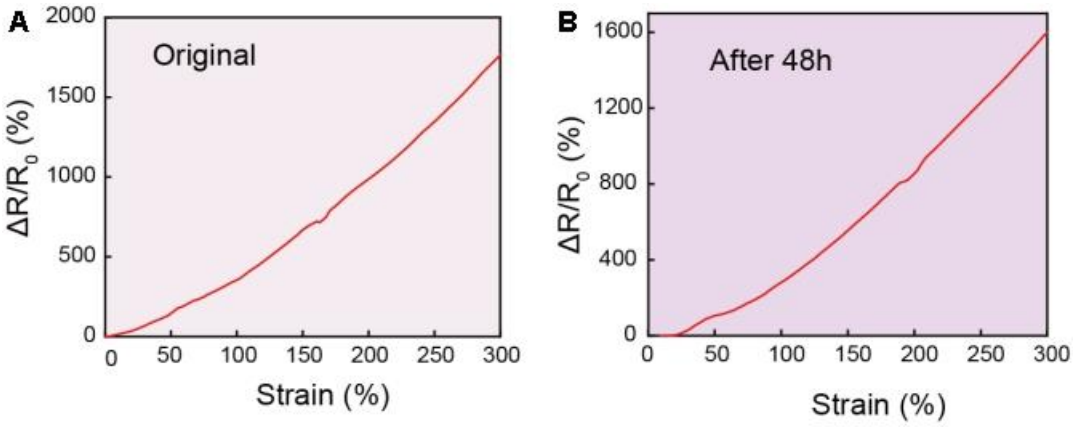

Supplementary Figure 10. The relative resistance change of freshly prepared hydrogel sensor (A) and hydrogel sensor stored for two days (B) at the same stimulated strain.

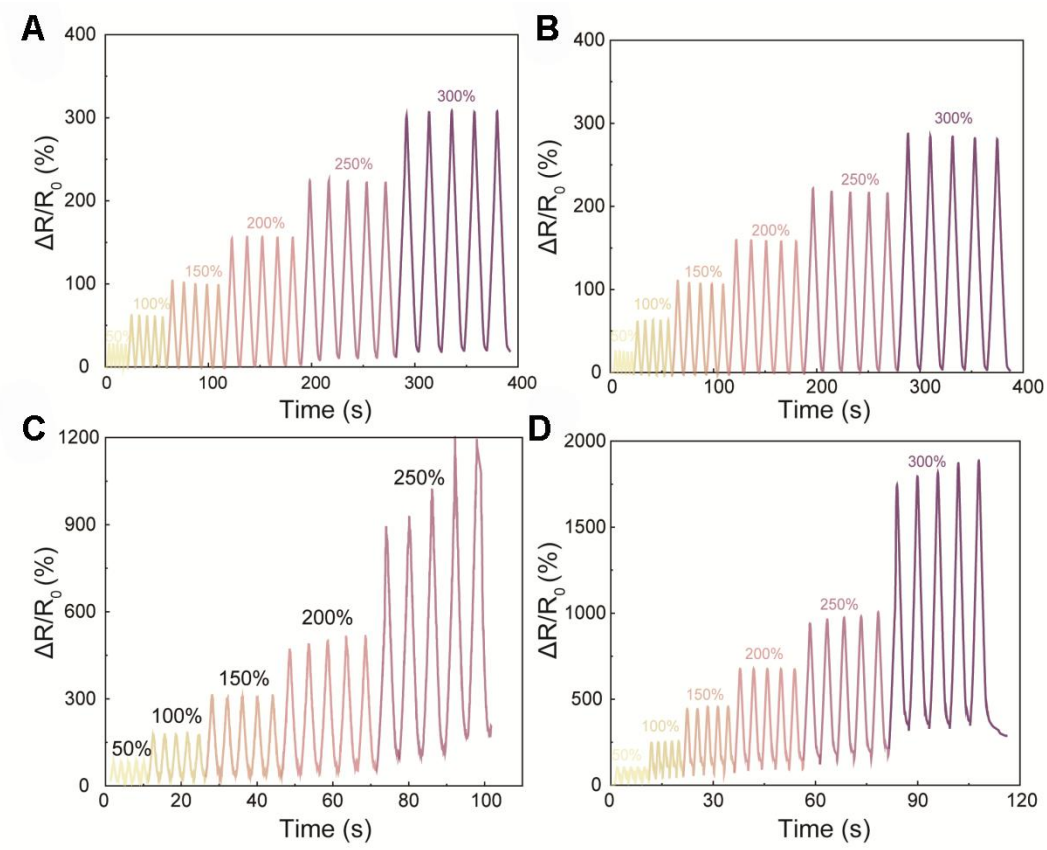

Supplementary Figure 11. Relative resistance variation of all 3D printed strain sensing devices with different pattern shapes over the 0-300% strain range, (A) Microwave pattern; (B) Curved line; (C) Rhombic; (D) Square.

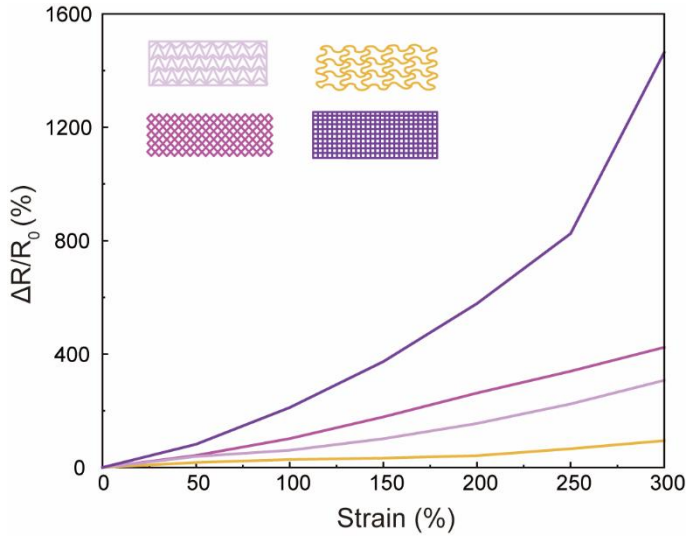

Supplementary Figure 12. Comparison of the sensitivity of fully 3D printed strain sensing devices with different pattern shapes, with four colors corresponding to four patterns.

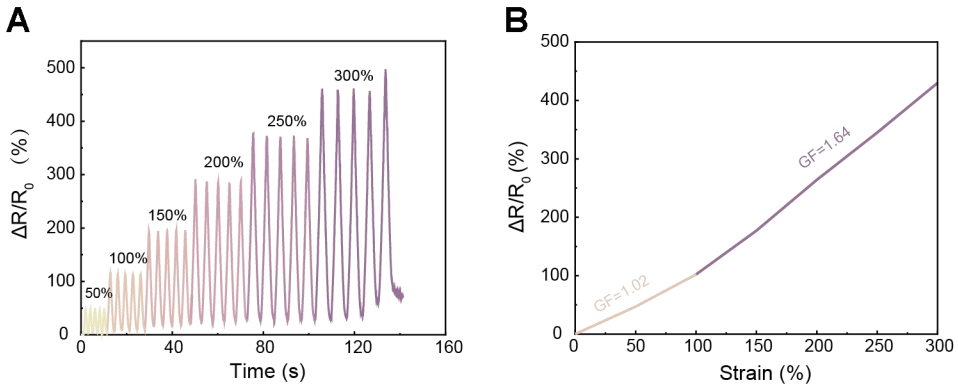

Supplementary Figure 13. (A) Variation of the relative resistance of the planar structure strain sensor over different strain ranges (0-300%). (B) GF curves of plane structure strain transducers at different strains.

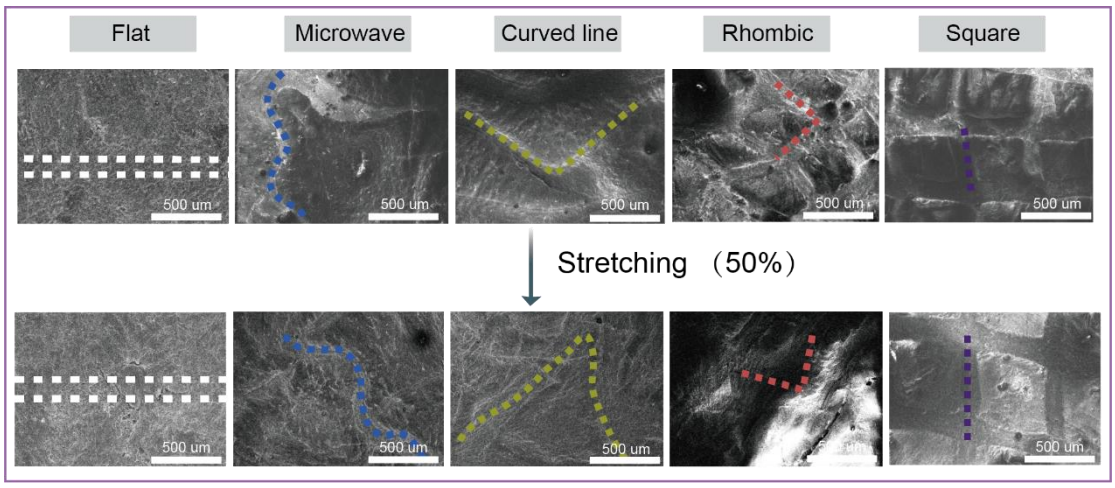

Supplementary Figure 14. Scanning electron microscopy images of different structural PEDOT:PSS-PVA hydrogels (Scale bar: 500 μm, The dotted line represents the conductive path).

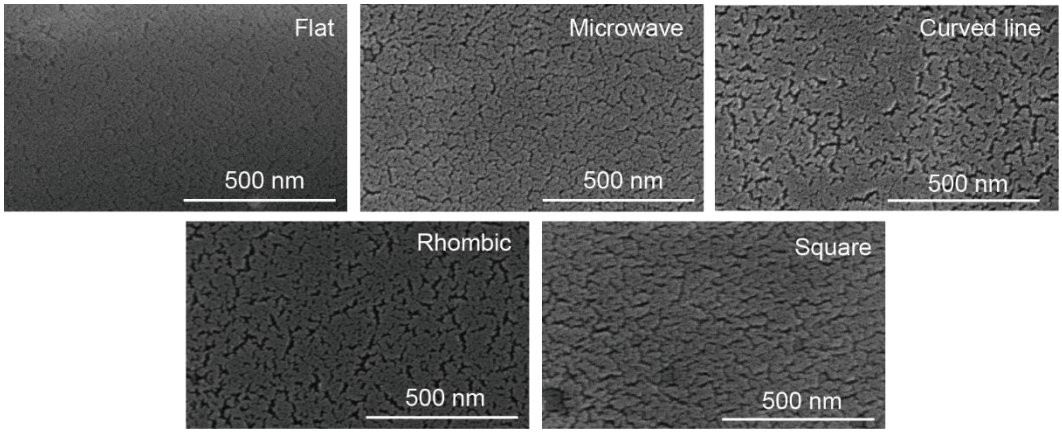

Supplementary Figure 15. Microcracks images of different structural PEDOT:PSS-PVA hydrogels, under 50% nominal strain. (Scale bar: 500 nm)

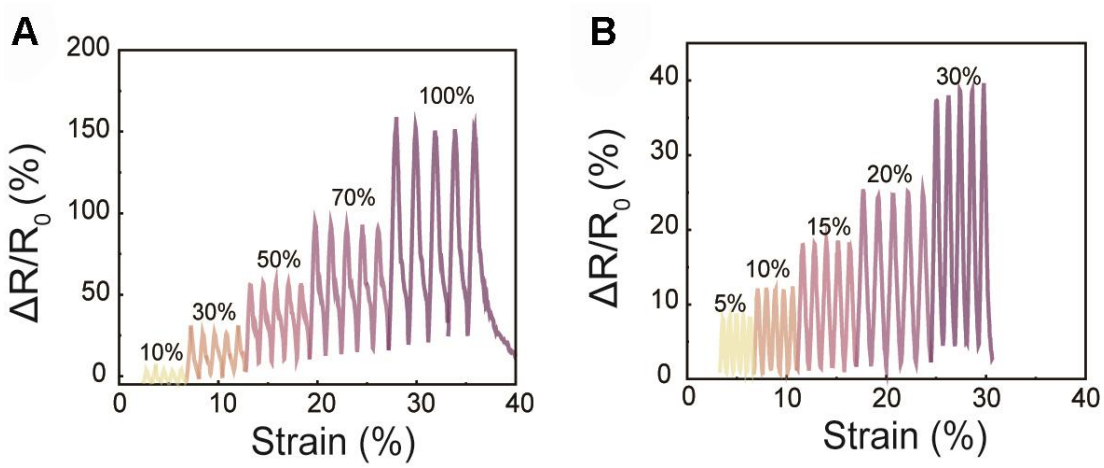

Supplementary Figure 16. Relative resistance change of all 3D-printed square strain sensing devices in (A) the medium strain range (10%-100%) and (B) the small strain range (5%-30%).

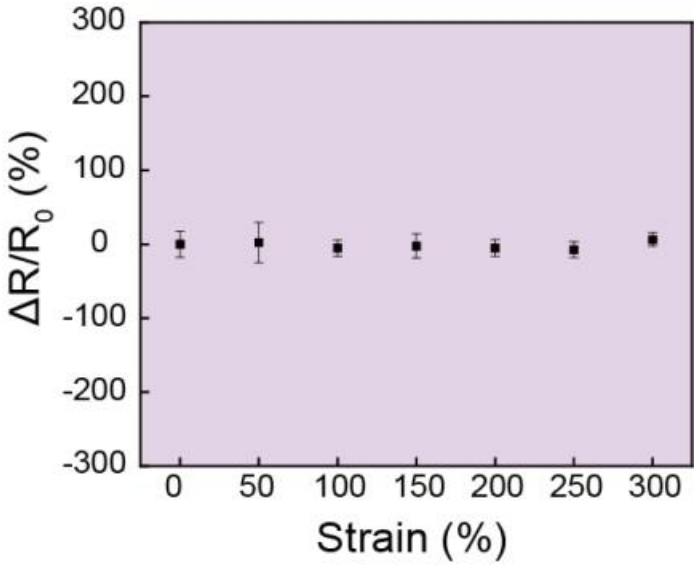

Supplementary Figure 17. The relative change in longitudinal resistance under different ranges of lateral stretching strain (0-300%).

Supplementary Table 1. Comparison of all 3D-printed PEDOT:PSS/PVA hydrogel strain sensing device with previously reported PEDOT/PVA-based strain sensors

Main component	Stretchability	Sensitivity (GF)	Cycle stability	References
PEDOT:PSS/PVA/PAA	300%	3.82	100 cycles (100% strain)	J. Colloid Interface Sci. 2022, 618, 111-120
PEDOT:PSS/PVA/Mxene/PDA	500%	2.55	2000 cycles (50% strain)	J. Mater. Chem. A 2021, 9, 22082
PEDOT/PVA/PAA	400%	1.18	N/A	Polymer 2020, 196, 122469
PEDOT:PSS/PVA/Sisal	7%	3.98	100 cycles (3% strain)	Sensors 2021, 21, 4083.
PEDOT:PSS/PVA	300%	4.07	2000 cycles (100% strain)	Adv. Mater. 2022, 34, 2203650
PEDOT:PSS/PVA	100%	4.4	N/A	Polym. Test. 2020, 81, 106213
PAANa/PEDOT:PSS/PVA	200%	0.989	10 cycles (50% strain)	Mater. Today Commun. 2022, 33, 104324
PEDOT:PSS/PVA	130%	5.4	3000 cycles (10% strain)	ACS Appl. Mater. Interfaces 2022, 14, 35114-35125
PEDOT:PSS/PVA	300%	12.78	3000 cycles (100% strain)	This work